



**HAL**  
open science

## Sepal shape variability is robust to cell size heterogeneity in Arabidopsis

Duy-Chi Trinh, Claire Lionnet, Christophe Trehin, Olivier Hamant

► **To cite this version:**

Duy-Chi Trinh, Claire Lionnet, Christophe Trehin, Olivier Hamant. Sepal shape variability is robust to cell size heterogeneity in Arabidopsis. *Biology Letters*, 2024, 20 (5), pp.20240099. 10.1098/rsbl.2024.0099 . hal-04694502

**HAL Id: hal-04694502**

**<https://hal.inrae.fr/hal-04694502v1>**

Submitted on 10 Jan 2025

**HAL** is a multi-disciplinary open access archive for the deposit and dissemination of scientific research documents, whether they are published or not. The documents may come from teaching and research institutions in France or abroad, or from public or private research centers.

L'archive ouverte pluridisciplinaire **HAL**, est destinée au dépôt et à la diffusion de documents scientifiques de niveau recherche, publiés ou non, émanant des établissements d'enseignement et de recherche français ou étrangers, des laboratoires publics ou privés.



**HAL**  
open science

## Sepal shape variability is robust to cell size heterogeneity in Arabidopsis

Duy-Chi Trinh, Claire Lionnet, Christophe Trehin, Olivier Hamant

► **To cite this version:**

Duy-Chi Trinh, Claire Lionnet, Christophe Trehin, Olivier Hamant. Sepal shape variability is robust to cell size heterogeneity in Arabidopsis. *Biology Letters*, 2024, 20 (5), 10.1098/rsbl.2024.0099 . hal-04691144

**HAL Id: hal-04691144**

**<https://hal.science/hal-04691144v1>**

Submitted on 7 Sep 2024

**HAL** is a multi-disciplinary open access archive for the deposit and dissemination of scientific research documents, whether they are published or not. The documents may come from teaching and research institutions in France or abroad, or from public or private research centers.

L'archive ouverte pluridisciplinaire **HAL**, est destinée au dépôt et à la diffusion de documents scientifiques de niveau recherche, publiés ou non, émanant des établissements d'enseignement et de recherche français ou étrangers, des laboratoires publics ou privés.

1 **Sepal shape variability is robust to cell size variability in Arabidopsis**

2 Duy-Chi Trinh<sup>1,2,\*</sup>, Claire Lionnet<sup>1</sup>, Christophe Trehin<sup>1</sup>, and Olivier Hamant<sup>1,\*</sup>

3 <sup>1</sup> Laboratoire de Reproduction et Développement des Plantes, Université de Lyon, ENS de Lyon,  
4 UCBL, INRAE, CNRS, 46 Allée d'Italie, 69364 Lyon Cedex 07, France

5 <sup>2</sup> University of Science and Technology of Hanoi. Vietnam Academy of Science and Technology  
6 (VAST), 18 Hoang Quoc Viet, Cau Giay, Ha Noi, Vietnam

7 \* Duy-Chi Trinh, Olivier Hamant

8 Laboratoire de Reproduction et Développement des Plantes, Université de Lyon, ENS de Lyon,  
9 UCBL, INRAE, CNRS, 46 Allée d'Italie, 69364 Lyon Cedex 07, France

10 Email: duy-chi.trinh@ens-lyon.fr, olivier.hamant@ens-lyon.fr

11 **Main conclusion**

12 A mixed population of cells with varied sizes plays a limited role in ensuring the symmetrical  
13 shape of the sepal, and is not essential for sepal shape robustness in Arabidopsis.

14 **Abstract**

15 How organisms produce organs with robust shapes and sizes is still an open question. In recent  
16 years, the Arabidopsis sepal has been used as a model system to study this question because of its  
17 highly reproducible shape and size. One interesting aspect of the sepal is that its epidermis contains  
18 cells with very different sizes. Previous reports had qualitatively shown that sepals with more or  
19 less giant cells exhibit comparable final size and shape. Here we investigate this question using  
20 quantitative approaches. We find that a mixed population of cell size modestly contribute to the  
21 normal width of the sepal, but is not essential for its shape robustness. Furthermore, in a mutant  
22 with increased cell and organ growth variability, the change in final sepal shape caused by giant  
23 cells is exaggerated, but the shape robustness is not affected. This formally demonstrates that sepal  
24 shape variability is robust to cell size heterogeneity.

25 **Key words:** Paf1c, morphogenesis, growth, reproducibility, variability

## 26 **Introduction**

27 How organisms produce organs with robust shapes and sizes is one of the central mysteries of  
28 development in all kingdoms (Vogel, 2013). Cell size can have an ambiguous contribution to organ  
29 shape. There are examples where increasing cell size also increases organ shape, and others where  
30 increase in cell size is compensated (e.g. by decreasing cell number) (Horiguchi and Tsukaya,  
31 2011; Tabeta et al., 2023). In either case, how this affects the standard deviation in organ shape (a  
32 proxy for organ shape robustness) is ill-documented. This is what we study here.

33 The *Arabidopsis* sepal, the protective organ of a flower, offers an excellent model to answer that  
34 question because of its highly reproducible shape and size and easy access, among other reasons  
35 (Roeder, 2021). The sepal initiates from a flower meristem, and quickly grows following a well-  
36 documented pattern of cell growth and division (Hervieux et al., 2016; Trinh et al., 2023; Zhu et  
37 al., 2020).

38 Using this model, several possible mechanisms for shape robustness have been put forward. These  
39 mechanisms may be at the whole organ scale, such as timing of initiation and growth arrest (Zhu  
40 et al., 2020; Hervieux et al., 2016). They may also involve activities at the cellular scale, such as  
41 the constant reorientation of cell growth direction to achieve a robust average one, or the  
42 mechanical shielding of cells neighboring fast-growing ones (Hong et al., 2016; Hervieux et al.,  
43 2017). Recently, we investigated the possible impacts of increased transcriptional noise to shape  
44 robustness using a mutant of VERNALIZATION INDEPENDENCE 3 (VIP3), a subunit of the  
45 Polymerase-associated factor 1 complex (Paf1C). In the *vip3-1* mutant, transcriptional noise and  
46 growth rates between neighboring cells are more variable compared to the WT (Trinh et al., 2023).  
47 This increased local growth heterogeneity interferes with the formation of the large-scale growth  
48 pattern typically seen in the WT sepals, manifested as a delayed growth arrest at the sepal tip of  
49 the *vip3* mutant (Hervieux et al., 2016; Trinh et al., 2023).

50 The epidermal layer of a sepal consists of cells of vastly different size, which are usually divided  
51 into two different cell types: smaller cells and giant cells. Smaller cells are the product of frequent  
52 cell division, while giant cells result from early termination of cell division and subsequent  
53 endoduplication (Roeder, 2021; Roeder et al., 2010, 2012). Giant cells are very long cells that can  
54 extend from the base to the tip of the sepal, and they are usually quite straight (Meyer et al., 2017;

55 Mollier et al., 2023). Despite the variability in cell sizes and growth rates, all cells experience a  
56 similar sigmoid curve where growth is initially slow, then accelerate, and then slow down again,  
57 and they all reach the same maximum of growth rate, albeit at different times (Tauriello et al.,  
58 2015). Past studies have shown that the sepals in the wild type and mutants do not differ majorly,  
59 whether the mutant epidermis lacks giant cells or instead, is made up of giant cells only (Roeder  
60 et al., 2010; Robinson et al., 2018). However, the aspect of shape robustness was not characterized  
61 quantitatively, hence whether more subtle effects are induced when the ratio of giant vs. small  
62 cells is affected remains to be investigated. This is what we investigate here, also testing the  
63 response in a mutant where mechanisms for shape robustness are compromised.

## 64 **MATERIALS AND METHODS**

### 65 **Plant materials and growth conditions**

66 All experiments were performed on Col-0 ecotype. The *vip3-1* (Salk\_139885) mutant is described  
67 in (Fal et al., 2017), and the *pATML1::LGO* line in (Roeder et al., 2010).

68 Plants were grown on soil 20°C in short-day conditions (8h light/16h dark) for 3 weeks then  
69 transferred to long-day conditions (16h light/8h dark cycle).

### 70 **Sepal parameter measurements**

71 To compare sepals of different phenotypes, mature flowers of stage 14 as described in (Smyth et  
72 al., 1990) were used. The abaxial sepals were removed from the flowers and placed as flat as  
73 possible on double-sided tape on a microscope slide, over a black background. The images were  
74 taken with a Leica binocular equipped with a camera. To extract sepal contours and morphological  
75 parameters such as length, width and aspect ratio, the program called SepalContour was used as  
76 originally described in (Hong et al., 2016).

### 77 **Quantification of sepal shape variability**

78 To quantify shape variability from the sepal contours extracted by the SepalContour tool, another  
79 program called Contour Analysis also originally described in (Hong et al., 2016) was used. For a  
80 given genotype, the contours of all abaxial sepals were normalized to their area, and an average  
81 contour is calculated. The squared deviation of each contour from the average contour is then

82 calculated ( $S_2$  value). These  $S_2$  values were used to report shape variability of sepals (higher values  
83 mean more variable shape).

#### 84 **The maximal width position of the sepal**

85 The maximal width position (MWP) of the sepal is defined as the position along the sepal where  
86 its width is largest. To identify this position, an ImageJ macro was written to scan along the sepal  
87 contour (a product of the SepalContour tool) and identify the sepal length as well as the maximal  
88 width position. This position is relative to the length of the sepal and is expressed in percentage.

#### 89 **SEM images of sepals**

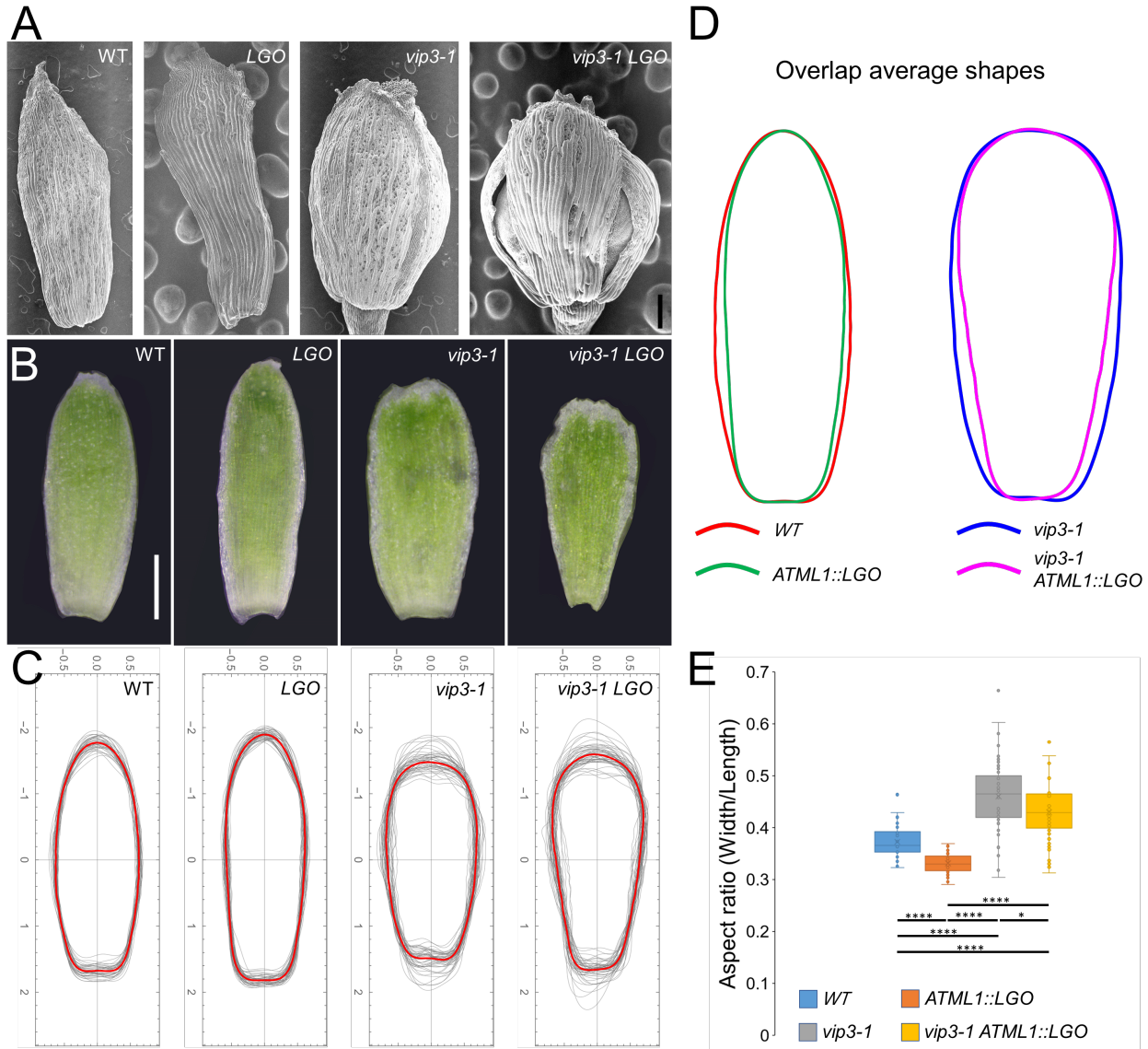
90 Scanning electron microscope (SEM) images of sepals were taken with a HIROX SH3000 tabletop  
91 microscope.

92

### 93 **RESULTS AND DISCUSSION**

94 To check whether a mix population of small and giant cells seen in the wild-type sepal is essential  
95 for its shape, we used the transgenic line *pATML1::LGO* where epidermal cells experience  
96 endoreduplication to become giant cells. *LGO* (*LOSS OF GIANT CELLS FROM ORGANS*)  
97 encodes a cyclin-dependent kinase inhibitor, while the *ATML1* (*MERISTEM LAYER 1*) promoter  
98 drives the expression specifically in the epidermis. While a wild-type sepal exhibits cells of various  
99 sizes, those expressing *pATML1::LGO* produce long giant cells which make up most of the  
100 epidermal cell population ([Figure 1A](#)) (Schwarz and Roeder, 2016). To analyze the effects of giant  
101 cell proportion on organ shape and shape variability, we used the SepalContour tool described in  
102 (Hong et al., 2016) to extract the contour as well as to measure the aspect ratio (width/length) of  
103 each sepal ([Figure 1B-C](#); lengths and widths in mm are provided in [Supplemental Table 1](#)). From  
104 all individual contours, an average contour and a score of shape variability ( $S_2$ ) are calculated  
105 (Hong et al., 2016; Trinh et al., 2023). The average contour means the average shape of the sepals  
106 in a given genotype. The shape variability tells us if individual sepals have similar or different  
107 shapes.

108 To better see the change in the sepal shape, we overlapped the average contour of wild-type and  
 109 *pATML1::LGO* sepals, and found that despite their vastly different cell populations, they are in  
 110 fact very similar in shape (Figure 1D, left). This is consistent with previous qualitative  
 111 observations (Roeder et al., 2010; Robinson et al., 2018).



112

113 **Figure 1. The effects of giant cells on sepal shape**

114 (A) Scanning electron microscopy pictures of wild-type, *pATML1::LGO* (*LGO*), *vip3-1* and *vip3-1*  
 115 *pATML1::LGO* (*vip3-1 LGO*) sepals. Giant cells make up most of the outer epidermal cell  
 116 population in *LGO* and *vip3-1 LGO* sepals. Scale bar = 200 μm.

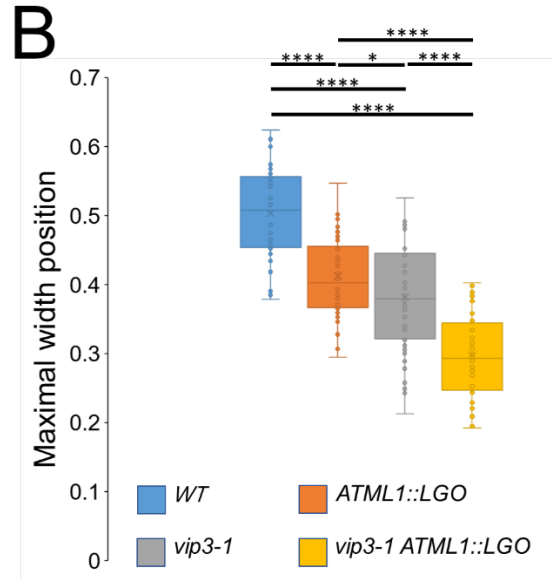
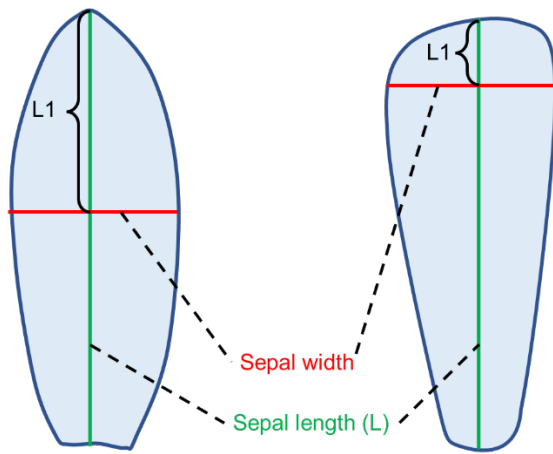
117 (B) Representative images of mature wild-type, *pATML1::LGO* (*LGO*), *vip3-1* and *vip3-1*  
118 *pATML1::LGO* (*vip3-1 LGO*) sepals. Scale bar = 0.5mm.  
119 (C) Plots showing the contours of sepals of the four genotypes. The contours are normalized to the  
120 area. The red outlines are the average shapes. n = 40, 48, 50, 53 sepals for wild type,  
121 *pATML1::LGO* (*LGO*), *vip3-1* and *vip3-1 LGO*, respectively.  
122 (D) Overlapping average shapes of wild type and *pATML1::LGO* (upper half), and of *vip3-1* and  
123 *vip3-1 LGO* (lower half).  
124 (E) Aspect ratios (width/length) of sepals of the four genotypes. A higher aspect ratio means a  
125 wider shape, and *vice versa*. n = 40, 48, 50, 53 sepals for wild type, *pATML1::LGO* (*LGO*), *vip3-*  
126 *1* and *vip3-1 LGO*, respectively. Welch's t-test. Asterisks indicate level of statistical significance:  
127 \*  $p \leq 0.05$ , \*\*  $p \leq 0.01$ , \*\*\*  $p \leq 0.001$ , \*\*\*\*  $p \leq 0.0001$ .

128

129 We also found that *pATML1::LGO* sepals were slightly narrower, when compared to the wild type,  
130 as evidenced by a lower aspect ratio (0.37 for wild type and 0.33 for *pATML1::LGO*, [Figure 1E](#)).  
131 The narrowing of the *pATML1::LGO* sepals was more pronounced near the middle of the sepal.  
132 To characterize this change, we identified the maximal width position (MWP) of the sepal, which  
133 is the position along the sepal where its width is largest. A score greater than 0.5 means that the  
134 sepal is widest at a position closer to the sepal base, while a MWP smaller than 0.5 means that the  
135 sepal is widest closer to the tip. This MWP index can distinguish between two shapes of the same  
136 aspect ratio and is a potentially useful morphological parameter ([Figure 2A](#)). An ImageJ macro  
137 was written to scan along the sepal contour (a product of the SepalContour tool) and identify the  
138 sepal length as well as the MWP. Using this index, we found that the wild type produces symmetric  
139 sepals with the MWP around the middle. Consistent with what we noticed, the MWP index of the  
140 *pATML1::LGO* line is lower than that of the wild type ( $MWP_{WT} = 0.50$ ,  $MWP_{ATML1::LGO} = 0.41$ ,  
141 [Figure 1G](#)), meaning that the MWP of *ATML1::LGO* sepals is in the middle, closer to the tip.  
142 Because these modifications remain minor, this analysis rather confirms that sepal shape is robust  
143 to cell size perturbation.



**A**  
 $L1/L = \text{Maximal Width Position}$



144

145 **Figure 2.** The Maximal width position index to quantify the effects of giant cells on sepal shape

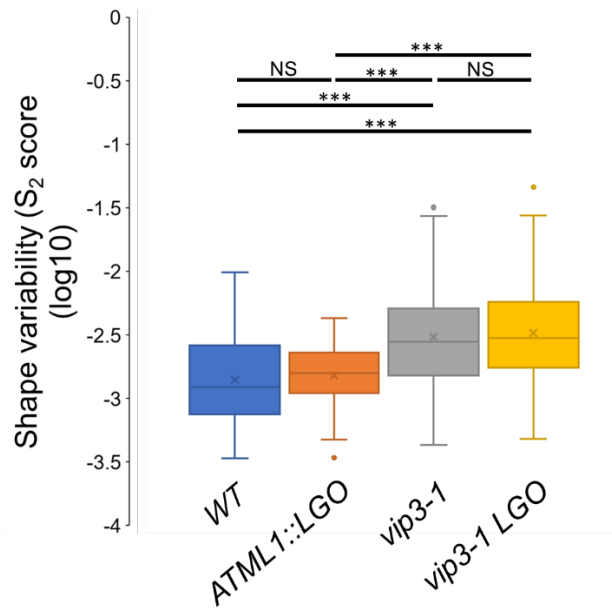
146 (A) Two shapes of the same aspect ratio can be vastly different. To distinguish them, we identify  
 147 the Maximal width position (MWP) where the width is widest along the sepal length. The ratio  
 148  $L1/L$  is the MWP index, with  $L$  being the sepal length, and  $L1$  being the distance from the tip to  
 149 the MWP.

150 (B) Maximal width position (MWP) index of sepals of the four genotypes. A lower MWP index  
 151 means the sepal is widest near the tip.  $n = 40, 48, 50, 53$  sepals for wild type, *ATML1::LGO* (*LGO*),  
 152 *vip3-1* and *vip3-1 LGO*, respectively. 2-sided Welch's t-test. Asterisks indicate level of statistical  
 153 significance: \*  $p \leq 0.05$ , \*\*  $p \leq 0.01$ , \*\*\*  $p \leq 0.001$ , \*\*\*\*  $p \leq 0.0001$ .

154

155

156 Yet similar shape averages do not necessarily mean similar standard deviation. To check whether  
 157 more giant cells in sepals make them more or less variable in shape, we calculated shape variability  
 158 ( $S_2$  score expressing the squared deviation of sepal contours from the average contour) using the  
 159 SepalContour tool. We found that wild type and *pATML1::LGO* sepals essentially have the same  
 160 level of variability ( $S_2$  score as median  $\pm$  SE =  $1.21 \pm 0.29 \cdot 10^{-3}$  for wild type, =  $1.52 \pm 0.15 \cdot 10^{-3}$   
 161 for *ATML1::LGO*) (Figure 3). The data shows that sepals with only one type of cells (giant cells)  
 162 can still exhibit wild-type-level shape variability.



163

164 **Figure 3.** Sepal shape variability quantification in the wild type and lines with different mix of  
 165 cell sizes

166 Sepal shape variability is expressed as S<sub>2</sub> score (squared deviation of sepal contours from the  
 167 average contour) in log10 scale to aid with visualization. Higher score means higher shape  
 168 variability. n = 40, 48, 50, 53 sepals for wild type, *pATML1::LGO* (*LGO*), *vip3-1* and *vip3-1 LGO*,  
 169 respectively. 2-sided Welch's t-test. Asterisks indicate level of statistical significance: \*  $p \leq 0.05$ ,  
 170 \*\*  $p \leq 0.01$ , \*\*\*  $p \leq 0.001$ , \*\*\*\*  $p \leq 0.0001$ . NS: not significant.

171

172 The presence of giant cells could alter sepal shape in a couple of ways. First, giant cell precursors  
 173 stop dividing early, so the number of cells or cell files across the sepal may be reduced, leading to  
 174 a narrower shape. Second, because giant cells are usually long and straight, they can potentially  
 175 influence the shape of the whole sepal, much like the ribs of a hand fan make the fan's shape.  
 176 Nevertheless, the effects of giant cells on the sepal shape in the wild-type background is quite  
 177 small, probably because local growth, *i.e.* at the wall scale, is not majorly affected (Tauriello et al.,  
 178 2015) and because global mechanisms channel growth pattern, for example, proper growth arrest  
 179 at the sepal tip (Hervieux et al., 2016; Trinh et al., 2023).

180 To further check the contribution of giant cells to sepal shape, we used a background where  
 181 mechanisms for proper sepal growth are compromised. In the *vip3-1* mutant, gene expression

182 becomes more variable, leading to increased variability in molecular growth regulators (ROS,  
183 auxins), increased local growth heterogeneity, and increased shape variability (Trinh et al., 2023).  
184 We reasoned that, in *vip3-1*, we might uncover stronger effects of giant cell overpopulation on  
185 final sepal shape. *vip3-1* sepals have a mixed of cell population, which is comparable to wild-type  
186 ones (Figure 1A). In wild-type sepals, the sepal tip stops growing early during sepal development,  
187 but that of *vip3-1* sepals keeps growing for longer (Trinh et al., 2023). To check our hypothesis,  
188 we introduced *pATML1::LGO* into the *vip3-1* background and measured sepal shape and shape  
189 variability (Figure 1A-C).

190 First, we extracted the average shape of *vip3-1* and *vip3-1 LGO* (*vip3-1 ATML1::LGO*) sepals and  
191 overlapped their average shapes (Figure 1D, right). *vip3-1* sepals were significantly wider than  
192 those of the wild type, as previously shown (Figure 1D-E; (Trinh et al., 2023)). Regarding the  
193 contribution of giant cells to average sepal shape, we found that, as in the wild type, they make  
194 *vip3-1* sepals significantly narrower mostly at the lower half of the sepal (towards the base),  
195 leading to a slightly lower aspect ratio (0.46 for *vip3-1* and 0.43 for *vip3-1 LGO*; Figure 1D-E).  
196 To further understand this change, we measured the MWP index and found that while  
197 *pATML1::LGO* and *vip3-1* sepals have the MWPs similarly closer to the tip ( $MWP_{35S::LGO} = 0.40$ ,  
198  $MWP_{vip3-1} = 0.38$ , 5% difference), that of *vip3-1 LGO* is pushed significantly further to the tip  
199 ( $MWP_{vip3-1 LGO} = 0.30$ , 21% difference compared to  $MWP_{vip3-1}$ ) (Figure 2B). The large change in  
200 shape observed in *vip3-1 LGO* double mutant supports our hypothesis that the effects of giant cells  
201 would be exaggerated in a mutant with compromised mechanisms for organ growth.

202 We then calculated the score for sepal shape variability. Surprisingly, we found that there is no  
203 significant difference in shape variability between *vip3-1* and *vip3-1 LGO* sepals, i.e. similar to  
204 the comparison between wild-type and *pATML1::LGO* sepals ( $S_2$  score as median  $\pm$  SE =  $2.78 \pm$   
205  $1.0 \cdot 10^{-3}$  for *vip3-1*, =  $2.94 \pm 1.1 \cdot 10^{-3}$  for *vip3-1 LGO*) (Figure 3). This further confirms that sepal  
206 shape variability is robust to cell size heterogeneity. Note that since *vip3-1* already exhibits high  
207 shape variability, we cannot completely rule out the possibility that it is difficult to induce even  
208 higher variability by changing cell types.

209 Recently, another team was also independently investigating the roles of cell types in sepal shape  
210 robustness (Burda et al., 2023). They showed that sepals having only giant cells (*pATML1::LGO*)

211 or small cells (*lgo* mutant) have similar shape robustness compared to wild-type sepals (Burda et  
212 al., 2023), consistent with our results here. Using time-lapse imaging to analyze growth pattern at  
213 cellular level of wild-type, *pATML1::LGO* and *lgo* sepals, they associated their similar shape  
214 robustness with a similar cell growth pattern. When they introduced these lines into *ftsh4-5*  
215 (*filamentous temperature sensitive H 4*), a mutant with reduced shape robustness, they found that  
216 a population of small cells only (*lgo ftsh4-5*) significantly increase sepal shape variability in the  
217 *ftsh4-5* background, while giant cells (*pATML1::LGO ftsh4-5*) did not. The increase in sepal shape  
218 variability was associated with uneven growth rates and disorganized growth directions of cells  
219 (Burda et al., 2023). Overall, their findings are complementary to ours, and provide a cell growth-  
220 based explanation for shape robustness of the mutants.

221 To summarize, our quantitative analyses reveal that: (i) a diverse cell population is not necessary  
222 for robust sepal shape, as demonstrated by similar shape variability between wild type and  
223 *pATML1::LGO*, (ii) while giant cells do not change shape variability, they could alter sepal shape  
224 in a subtle way, and (iii) in a background where growth variability is promoted and shape  
225 robustness is compromised (*vip3-1*), giant cells could induce more pronounced change in shape,  
226 but still did not affect shape variability. This suggests that organ shape variability does not emerge  
227 at the cell scale, but rather at smaller scales (e.g. individual cell wall properties, e.g. (Tauriello et  
228 al., 2015)) or larger scales (clones of cells, (Tsugawa et al., 2017)). This means that the question  
229 of how organs know when to stop growing should be addressed with a multiscale lens.

### 230 **Data accessibility**

231 The datasets analyzed during the current study, the code used to identify the Maximal width  
232 position in ImageJ, and the supplemental table 1 are available from the OSF repository:  
233 <https://osf.io/4aep5/>.

234

### 235 **Declaration of AI use**

236 We have not used AI-assisted technologies in creating this article.

237

### 238 **Author contributions:**

239 D-C.T, C.T and O.H designed research; D-C.T conducted experiments and analyzed data; D-C.T  
240 prepared the original paper draft; C.L. wrote the ImageJ macro. All authors read and approved the  
241 manuscript.

242 **Competing Interest Statement:** The authors declare no competing interest.

243 **Acknowledgements:**

244 We thank Dr. Adrienne Roeder (Cornell University, Ithaca, New York, USA) for *pATML1::LGO*  
245 seeds and for critical reading of the manuscript. We thank PLATIM platform for their help in using  
246 the Hirox microscope. This work is supported by the European Research Council (ERC, grant  
247 agreement No 101019515, “Musix”), by CEFIPRA (grant 6103-1), and by the French National  
248 Research Agency through a European ERA-NET Coordinating Action in Plant Sciences (ERA-  
249 CAPS) grant (Grant No. ANR-17-CAPS-0002-01).

250

251 **References**

- 252 **Burda, I., Li, C.-B., Clark, F.K., and Roeder, A.H.K.** (2023). Robust organ size in  
253 Arabidopsis is primarily governed by cell growth rather than cell division patterns. bioRxiv:  
254 2023.11.11.566685.
- 255 **Fal, K., Liu, M., Duisembekova, A., Refahi, Y., Haswell, E.S., and Hamant, O.** (2017).  
256 Phyllotactic regularity requires the Paf1 complex in Arabidopsis. *Development* **144**: 4428–  
257 4436.
- 258 **Hervieux, N., Dumond, M., Sapala, A., Routier-Kierzkowska, A.L., Kierzkowski, D.,**  
259 **Roeder, A.H.K., Smith, R.S., Boudaoud, A., and Hamant, O.** (2016). A Mechanical  
260 Feedback Restricts Sepal Growth and Shape in Arabidopsis. *Curr. Biol.* **26**: 1019–1028.
- 261 **Hervieux, N., Tsugawa, S., Fruleux, A., Dumond, M., Routier-Kierzkowska, A.L.,**  
262 **Komatsuzaki, T., Boudaoud, A., Larkin, J.C., Smith, R.S., Li, C.B., and Hamant, O.**  
263 (2017). Mechanical Shielding of Rapidly Growing Cells Buffers Growth Heterogeneity and  
264 Contributes to Organ Shape Reproducibility. *Curr. Biol.* **27**: 3468-3479.e4.
- 265 **Hong, L. et al.** (2016). Variable Cell Growth Yields Reproducible Organ Development through  
266 Spatiotemporal Averaging. *Dev. Cell* **38**: 15–32.
- 267 **Horiguchi, G. and Tsukaya, H.** (2011). Organ size regulation in plants: Insights from  
268 compensation. *Front. Plant Sci.* **2**: 1–6.
- 269 **Meyer, H.M. et al.** (2017). Fluctuations of the transcription factor *atml1* generate the pattern of  
270 giant cells in the arabidopsis sepal. *Elife* **6**: 1–41.
- 271 **Mollier, C. et al.** (2023). Spatial consistency of cell growth direction during organ  
272 morphogenesis requires CELLULOSE SYNTHASE INTERACTIVE1. *Cell Rep.* **42**.
- 273 **Robinson, D.O., Coate, J.E., Singh, A., Hong, L., Bush, M., Doyle, J.J., and Roeder, A.H.K.**  
274 (2018). Ploidy and Size at Multiple Scales in the Arabidopsis Sepal. *Plant Cell* **30**: 2308–  
275 2329.

276 **Roeder, A.H.K.** (2021). Arabidopsis sepals: A model system for the emergent process of  
277 morphogenesis. *Quant. Plant Biol.* **2**: e14.

278 **Roeder, A.H.K., Chickarmane, V., Cunha, A., Obara, B., Manjunath, B.S., and**  
279 **Meyerowitz, E.M.** (2010). Variability in the control of cell division underlies sepal  
280 epidermal patterning in Arabidopsis thaliana. *PLoS Biol.* **8**.

281 **Roeder, A.H.K., Cunha, A., Ohno, C.K., and Meyerowitz, E.M.** (2012). Cell cycle regulates  
282 cell type in the Arabidopsis sepal. *Dev.* **139**: 4416–4427.

283 **Schwarz, E.M. and Roeder, A.H.K.** (2016). Transcriptomic effects of the cell cycle regulator  
284 LGO in Arabidopsis sepals. *Front. Plant Sci.* **7**: 1–22.

285 **Smyth, D.R., Bowman, J.L., and Meyerowitz, E.M.** (1990). Early flower development in  
286 Arabidopsis. *Plant Cell* **2**: 755–767.

287 **Tabeta, H., Gunji, S., Kawade, K., and Ferjani, A.** (2023). Leaf-size control beyond  
288 transcription factors: Compensatory mechanisms. *Front. Plant Sci.* **13**: 1–12.

289 **Tauriello, G., Meyer, H.M., Smith, R.S., Koumoutsakos, P., and Roeder, A.H.K.** (2015).  
290 Variability and constancy in cellular growth of Arabidopsis sepals. *Plant Physiol.* **169**:  
291 pp.00839.2015.

292 **Trinh, D.-C., Martin, M., Bald, L., Maizel, A., Trehin, C., and Hamant, O.** (2023). Increased  
293 gene expression variability hinders the formation of regional mechanical conflicts leading to  
294 reduced organ shape robustness. *Proc. Natl. Acad. Sci.* **120**: 2017.

295 **Tsugawa, S., Hervieux, N., Kierzkowski, D., Routier-Kierzkowska, A.-L., Sapala, A.,**  
296 **Hamant, O., Smith, R.S., Roeder, A.H.K., Boudaoud, A., and Li, C.-B.** (2017). Clones  
297 of cells switch from reduction to enhancement of size variability in Arabidopsis sepals .  
298 *Development* **144**: 4398–4405.

299 **Vogel, G.** (2013). How Do Organs Know When They Have Reached the Right Size? *Science*  
300 (80-. ). **340**: 1156–1157.

301 **Zhu, M. et al.** (2020). Robust organ size requires robust timing of initiation orchestrated by  
302 focused auxin and cytokinin signalling. *Nat. Plants*.